http://dx.doi.org/10.5012/bkcs.2013.34.12.3715

Growth and Migration of BALB/3T3 Fibroblast Cells on Nano-engineered Silica Beads Surface

Jihee Kim, Prakash Chandra, Jiyoon Yang, and Seog Woo Rhee*

*Department of Chemistry, Kongju National University, Kongju 314-701, Korea. *E-mail: jisanrhee@kongju.ac.kr*
Received July 30, 2013, Accepted September 23, 2013

In this study, the behavior of cells on the modified surface, and the correlation between the modified substrates and the response of cells is described. A close-packed layer of nano-sized silica beads was prepared on a coverslip, and the adhesion, proliferation, and migration of BALB/3T3 fibroblast cells on the silica layer was monitered. The 550 nm silica beads were synthesized by the hydrolysis and condensation reaction of tetraethylorthosilicate in basic solution. The amine groups were introduced onto the surfaces of silica particles by treatment with 3-aminopropyltrimethoxysilane. The close-packed layer of silica beads on the coverslip was obtained by the reaction of the amine-functionalized silica beads and the (3-triethoxysilyl)propylsuccinic anhydride treated coverslip. BALB/3T3 fibroblast cells were loaded on bare glass, APTMS coated glass, and silica bead coated glass with the same initial cell density, and the migration and proliferation of cells on the substrates was investigated. The cells were fixed and stained with antibodies in order to analyze the changes in the actin filaments and nuclei after culture on the different surfaces. The motility of cells on the silica bead coated glass was greater than that of the cells cultured on the control substrate. The growth rate of cells on the silica bead coated glass was slower than that of the control. Because the close-packed layer of silica beads gave an embossed surface, the adhesion of cells was very weak compared to the smooth surfaces. These results indicate that the adhesion of cells on the substrates is very important, and the actin filaments might play key roles in the migration and proliferation of cells. The nuclei of the cells were shrunk on the weakly adhered surfaces, and the S1 stage in which DNA is duplicated in the cell dividing processes might be retarded. As a result, the rate of proliferation of cells was decreased compared to the smooth surface of the control. In conclusion, the results described here are very important in the understanding of the interaction between implanted materials and biosystems.

Key Words : Cell-surface interaction, Surface modification, Nano silica bead, Contact angle, Growth and migration of cells

Introduction

The modulation of surfaces with nanoscale topography is attractive for many *in vitro* and *in vivo* applications of biomaterials, including regenerative medicine, tissue engineering, medical implants, cell-based sensors, and high throughput arrays as well as for advances in the fundamental understanding of cell-surface interaction and cell biology.[1] The microenvironment of the surfaces of biomaterials directs a variety of the cellular functions such as adhesion, proliferation, migration, and gene expression, modulates phenotypic differentiation, and alters the responsiveness to extracellular signals.[2] A wide range of cellular responses such as acceleration of the movement of cells, cytoskeletal reorganization, and changes in gene expression have been reported by other researchers for the various topographies of the surfaces in order to evaluate the cell-based mechanisms.[3]

Recent developments in techniques to produce controlled and accurate nanotopography have been contributing to a new era in the interaction between cells and surfaces.[4] Several strategies such as chemical and plasma etching, grit blasting, and plasma spraying have been employed to create micro- and nanoscale topography on surfaces using photolithography and soft lithography techniques.[5-10] Foss *et al.* reported the effect of the surface nanotopography of materials.[11] They observed that the mechanical interactions between cells and their substrates clearly direct the organization and function of the cells using microfabricated arrays of elastomeric and microneedle-like posts. Tan *et al.* highlighted the potential importance of traction forces in dynamic biological relationships between the external and internal forces, and demonstrated the utility of this microfabricated system to explore the interactions which can regulate the important aspects of many processes, including cell spreading, polarization, division, and migration.[12] Even though well-ordered micro and nano features can be developed using photolithography techniques, the processes are very expensive and time consuming, and require intricate equipment. As alternative approaches, nanosphere lithography and nanopits have been developed.[13] Recently, synthetic silica nanoparticles have been used for the modification and nanoscale engineering of the surfaces of biomaterials, to investigate the interaction between cells and engineered biomaterials.[13] An advantage of silica as a culture substrate is that it may be readily modified in order to produce a range of materials with various functional groups, charge, roughness, chemistry, wettability,

topology, and porosity.[14-16] Surfaces coated with colloidal silica have been shown to inhibit the spreading and proliferation of mammalian cells with no adverse effects on cell viability.[17] It has been shown that different nanotopography influences the adsorption of proteins, the adhesion of cells, the proliferation of cells, and the synthesis and secretion of extracellular matrix (ECM) molecules *in vitro*.[18] Lipski *et al.* reported that there is a critical dimension of nanotopography which influences the function of cells, and that the threshold size of features for nano-mechanotransduction is cell-specific.[19] They reported that the nanoscale roughness of surfaces formed by silica nanoparticle assemblies (50-300 nm in diameter) on glass surfaces affected the cellular processes in a cell-specific manner; smaller surface features favored cell proliferation in comparison to larger features.[19] They also reported that silica particles of different sizes assembled on stainless steel and titanium foils have been shown to affect the growth and differentiation of human bone-marrow derived mesenchymal progenitor cells (MPC's).[20]

In this study, the synthesis and immobilization of modified silica nanospheres on a coverslip, the behavior of cells on the modified surface, and the correlation between the modified substrates and the response of cells is described. A close-packed layer of nano-sized silica beads was prepared on the coverslip, and the adhesion, proliferation, and migration of BALB/3T3 fibroblast cells on the silica layer was monitored in order to investigate the effect of nanoscale features on the adhesion, growth and migration of fibroblast cells.

Experimental

All chemicals were purchased from Sigma-Aldrich Chemical Co., USA), Junsei Chemical Co. (Japan), Molecular Probes (USA), Vector Laboratories Ltd. (USA), and Samchun Chemicals (Korea) and were of reagent grade and used without further purification.

Cleaning of Substrates. Glass coverslips (18 mm × 18 mm, Marienfeld Inc., Germany) were cleaned by immersion in 2% of aqueous Micro-90^{TM} cleaning solution (International Products Co., USA) at room temperature for 60 min and sonicated in cleaning solution for 60 min. The cleaned glass coverslips were repeatedly rinsed in deionized water (10 times) and dried. The glass coverslips were treated with oxygen plasma (Harrick Scientific, PDC-002 Plasma Cleaner; 30 W) before use.

Synthesis of Silica Beads. Silica nano beads were synthesized using a modified Stöber method according to published procedure.[21-23] Tetraethylorthosilicate (TEOS, Aldrich) solution (8.8 g of TEOS in 100 mL of ethanol) was slowly added to the mixture of 15 mL of aqueous ammonia solution (28-34%, Aldrich) and 85 mL of ethanol with magnetic stirring at spin rates of 500-1,000 rpm at room temperature. The resultant mixture was stirred for an additional 3 h with the same spin rate at room temperature. The solid product was separated from the substrate by centrifugation (4,000 rpm, 10 min; MF 300, Hanil Science Industrial), and was washed with ethanol three times. Sediment was dried in a convection oven at 60 °C for 24 h and then stored in a desiccator. The larger silica beads were obtained by the additional hydrolysis and condensation reaction of TEOS with silica seeds prepared in the previous step.

Modification of Silica Beads Using Silane Molecules. The surfaces of the nano silica beads were modified using silane molecules according to published procedure.[24,25] Silica beads (3 g) were added to the mixture of 60 mL of 95% ethanol and 3 mL of water in a 100 mL beaker and the mixture was treated with an ultrasonic cleaner for 30 min at room temperature to obtain silica suspension. To the ethanolic silica suspension, 0.45 mL of 3-aminopropyltrimethoxysilane (APTMS, Aldrich) was added and the mixture was stirred for 30 min at room temperature. The solid product was separated from the mixture by centrifugation (4,000 rpm, 10 min), and washed with ethanol three times to remove unreacted materials. Sediment was dried in a convection oven at 105 °C for 24 h and then stored in a desiccator.

Modification of Glass Coverslips Using Silane Molecules. The surfaces of the glass coverslips were modified using silane molecules according to published procedure.[26-28] Oxygen plasma treated coverslips were immersed in 20 mL of 0.01 M ethanolic solution of (3-triethoxysilyl)propylsuccinic anhydride (TESPSA, Gelest, Inc.), and the Petri dishes containing the coverslips were slowly shaken for 18 h using an orbital shaker (Jeio Tech, SK-300). After treatment the coverslips were rinsed in ethanol and were dried under a pressurized stream of nitrogen gas.

Immobilization of Silica Beads on the Coverslips. Silica beads treated with APTMS were immobilized on the TESPSA treated coverslips according to published procedure, to obtain a close-packed layer of silica beads on the coverslip.[28] APTMS treated silica beads (0.85 g) were added to 10 mL of ethanol and the mixture was treated with an ultrasonic cleaner for 10 min at room temperature to obtain silica suspension. *N*,*N*-Diisopropylethylamine (0.35 g) as a catalyst for the condensation reaction of amine and anhydride was added to the mixture with stirring. The mixture was poured onto the TESPSA treated glass coverslip and left for 8 h in a laminar flow hood. After treatment the coverslip was rinsed in ethanol three times and was dried in a laminar flow hood.

Patterning of Silane Molecules on the Glass Coverslips. A Polydimethylsiloxane (PDMS, Dow Corning, USA) piece, having the desired surface embossed patterns, was used as a stamp. The PDMS stamp was fabricated using rapid prototyping and soft lithography techniques.[29] The PDMS stamp was placed on the silane treated glass coverslip, pressed with a stainless steel weight (100 g/cm^2), and exposed to reactive oxygen plasma using a plasma cleaner for 10 min. The oxygen plasma treated coverslip was immersed in 0.01% hexane solution of octadecyltrichlorosilane (OTS, Aldrich) in order to coat the etched regions with OTS for 5 min, and was washed with isopropyl alcohol three times. The coverslip was then dried under a stream of air in a laminar flow hood. Finally, coverslips treated with OTS were heated at 105 °C

for 10 min to complete the formation of chemical bonds between the OTS and the glass substrate.

Culture of Fibroblast Cell. The mouse embryonic fibroblast cell line BALB/3T3 (Korean Collection for Type Cultures, KCTC) was cultured in low glucose Dulbecco's modified Eagles medium (DMEM, Invitrogen) supplemented with 10% fetal bovine serum (FBS, Invitrogen) and 1% penicillin-streptomycin (Sigma) in a humidified incubator (Sanyo Electric, Japan) at 37 °C with 5% CO_2. For the cell growth experiment, control and treated coverslips were placed in 100-mm Petri dishes and 10 mL of growth media were added to each dish. The cells with a density of 1×10^5 cells/mL were loaded on each substrate, the dead cells were removed by washing with fresh media and HBSS (Hank's balanced salt solution, Invitrogen) after 1 h, and then fresh growth media were added. Live cell images were captured by inverted microscope, Olympus IX71, equipped with a DP71 CCD camera. Images were collected at a regular interval of 12 h, and the numbers of cells were counted by image analyses software (Image Pro-Plus® version 7.0, Media Cybernetics, USA). For the cell migration experiment, control and treated coverslips were placed in a 6-well cell culture plate, and 3 mL of growth media were added to each well. The cells with a density of 1×10^5 cells/mL were loaded on each substrate, the dead cells were removed, and the substrates were washed with HBSS, and then fresh growth media were added. Cells were cultured on the motorized stage (Prior) of the inverted microscope equipped with DP71 CCD camera, and CO_2, moisture, and temperature controllers. Time-lapse images of cells were acquired every 1 min for 1 h. The migration tracks were tracked and analyzed using a software package, Image Pro-Plus® version 7.0.

Live/dead Cell Analysis. After washing with PBS, cells were stained using the kit components (4 μM ethidium homodimer-1 (EthD-1) and 2 μM calcein AM). After 30 min incubation at room temperature, cells were imaged using fluorescence microscopy with 10× objective (Olympus IX71 with appropriate filter settings).

Fixation, Immunocytochemistry and Other Staining Methods. Cells were fixed in 4% paraformaldehyde (Aldrich) for 15 min at 37 °C followed by washing with PBS (pH 7.2). Subsequently, cells were permeabilized with 0.5% Triton X-100 (Aldrich) in PBS for 5 min at 4 °C. They were then blocked with 1% bovine serum albumin (BSA, Sigma) in PBS for 5 min at 37 °C. The cells were further sequentially exposed to primary, secondary and tertiary antibodies: rhodamine-conjugated phalloidin (1:100 in 1% BSA/PBS, Molecular Probes, 37 °C, 1 h); biotin-conjugated antibody (1:50 in 1% BSA/PBS, monoclonal horse antimouse (IgG), Vector Laboratories Ltd., 37 °C, 1 h); FITC conjugated streptavidin tertiary antibody (1:50 in 1% BSA/PBS, Vector Laboratories Ltd., 4 °C, 30 min). After washing, a 4,6-diamidino-2-phenylindole (DAPI, Molecular Probes) solution in PBS was added to the cells, and held for 10 min at room temperature to counter stain the nuclei. A final wash was then given to the sample. The samples were mounted in a polyvinyl alcohol (PVA) mounting medium (Fluka) with 1,4-diazabicyclo[2.2.2]octane (DABCO) and then viewed *via* a fluorescence microscope with 100× objective.

Results and Discussion

Schematic Illustration of Formation of Close-packed Silica Beads for Cell Culture. Schematic illustration of the fabrication of a close-packed silica beads-immobilized coverslip, and culture of cells on the modified substrate is shown in Figure 1. Hydroxyl groups of the glass coverslip reacted with ethoxysilane groups of the TESPSA molecules to form covalent bonds between the glass coverslip and the TESPSA molecules.[28] The amine groups of APTMS-treated silica beads reacted with acid anhydride groups of the TESPSA coated coverslip to form amide bonds in the presence of a catalytic amount of *N*,*N*-diisopropylethylamine. As a result, the silica beads were immobilized on the TESPSA coated coverslip by the formation of covalent bonds.[29] Cells were loaded on the APTMS-modified silica beads immobilized on the glass coverslip, and the growth and migration of cells

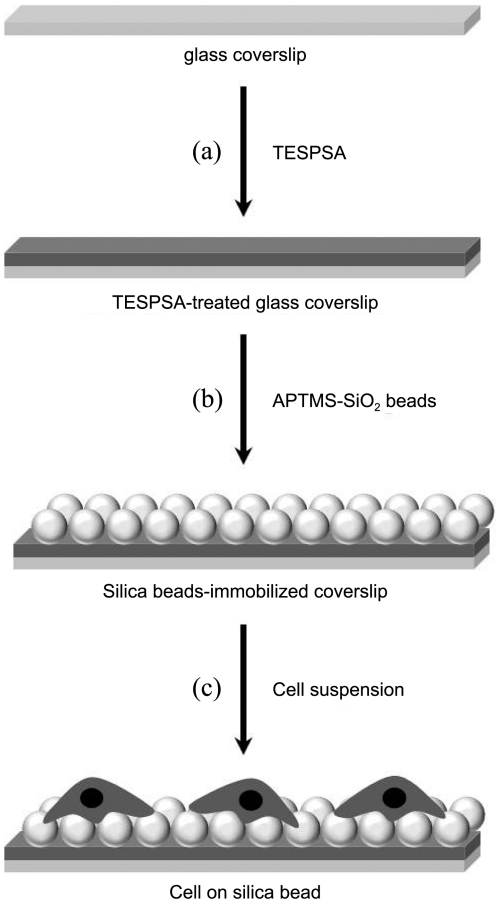

Figure 1. Schematic illustration of the fabrication of a close-packed silica beads-immobilized coverslip, and culture of cells on the modified substrate. (a) Glass coverslip was coated with TESPSA molecules. (b) APTMS-treated silica beads were immobilized on the TESPSA coated coverslip by the formation of covalent bond between amine group and acid anhydride group to give amide bond. (c) Cells were loaded on the APTMS-modified silica surface, and the growth and migration of cells were monitored by microscope at regular intervals.

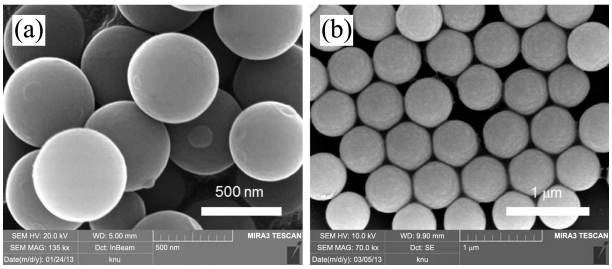

Figure 2. SEM images of silica beads. (a) silica beads as synthesized, (b) silica beads immobilized on the coverslip (top view). The monolayer of silica beads was formed with a close-packed structure. Average size of silica beads is 550 nm.

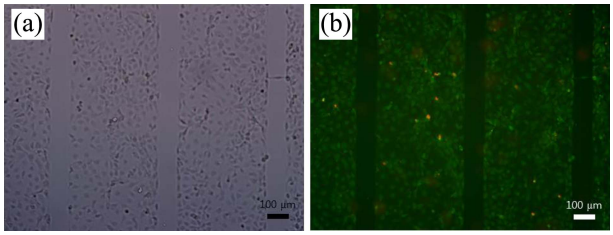

Figure 3. Microscopic images of patterned BALB/3T3 fibroblast cells cultured on the patterns of silica beads and OTS. (a) DIC images of cells, and (b) fluorescent microscopic images of cells treated with calcein AM and ethidium homodimer after culture for 24 h.

were monitored by microscope at regular intervals. Because the size of the silica beads and the thickness of the coatings were smaller than the wavelength of visible light, the resulting substrate was optically transparent, allowing the behavior of the cells to be monitored.

Close-packed Silica Beads on the Coverslip. The SEM images of the prepared silica beads are shown in Figure 2. The shape of prepared silica beads is spherical and the size of beads is highly uniform. The average particle size of beads is around 550 nm. The silica beads were highly ordered on the coverslip with a close-packed structure. Because the bonding between silica beads and coverslip is covalent, the silica beads were fixed on the substrate and maintained the close-packed structure during cell culture experiments. The monolayer of close-packed silica beads can supply the embossed surfaces for cell binding.

Patterning of Cells on the Close-packed Silica Beads on the Coverslip. BALB/3T3 fibroblast cells were cultured on the patterns of silica beads and OTS. Silica patterns were obtained using a piece of PDMS with channels (100 μm wide, separated by 400 μm spacing and 100 μm deep) on the coverslip. The entire assembly was exposed to oxygen plasma. After exposure to oxygen plasma, the coated areas not in contact with the patterning piece are completely etched away.[29] After immersion of the treated coverslip in the 0.01% hexane solution of OTS, a pattern of TESPSA coated area and OTS coated area is left. APTMS-treated silica beads were selectively immobilized on the TESPSA treated regions (Figure 3(a)).[28] Microscopic images of patterned BALB/3T3 fibroblast cells cultured on the silica patterns for 24 h are shown in Figure 3. When cells were added to the modified glass coverslip, they preferentially attached, spread, and proliferated on the regions of silica beads. No cells were observed on the region of OTS. Because the silica beads were coated with APTMS, the functional groups of the surfaces were propylamine ($-CH_2CH_2CH_2NH_2$) groups, which were partially protonated under the condition of cell culture.[30] The positively charged surfaces became hydrophilic with a water contact angle of 57°, and cells were able to attach on the region of silica beads. The OTS-treated area was hydrophobic with a water contact angle of 110° and non-adhesive to cells.[31]

The viability was assessed using calcein AM and ethidium homodimer live/dead stain. Live cells were brightly stained in green by calcein AM, while dead cells were brightly stained in red by ethidium homodimer. The viability was quantified by counting the different colored cells from the fluorescent microscopic images (Figure 3(b)) captured after culture for 24 h. The viability of cells was greater than 95%. This means that the silica beads-treated substrate is biocompatible for the culture of BALB/3T3 fibroblast cells.

Cell Migration. BALB/3T3 fibroblast cells were cultured on the three different types of substrate: bare glass coverslip as a control, APTMS-treated coverslip, and the silica beads coated coverslip. The cells with a density of 1×10^5 cells/mL were loaded on each substrate placed in each well of the 6-well plate, and cultured on the motorized stage of the inverted microscope. The cell migration was monitored by capture of time-lapse images of cells for 1 h with an interval of 1 min. Twenty independent experiments were performed in each case for a quantitative analysis of the cells. Each image was analyzed using Image Pro-Plus® software. 250 cells were analyzed for each substrate and superimposed migration tracks of 50 randomly selected cells from each substrate are shown in Figure 4. The cells exhibited clearly random movement on the substrates.

A significant difference in migration distances for fibroblast cells was observed. Average migration distances of cells for 1 min were 1.64 ± 1.29 mm on the bare glass, 1.72 ± 0.84 mm on the APTMS treated glass, and 2.31 ± 0.89 mm on the silica beads. Cells were attached most strongly on the "control" bare glass substrate compared to the other two substrates. Expression of actin drives cytoskeletal assembly and strongly promotes spreading. Therefore, cells cultured on the bare glass coverslip migrated slowly. Cells cultured on the APTMS treated glass were attached moderately on the substrate, the cells migrated slightly faster than those on the bare glass.

Both substrates gave flat smooth surfaces for attachment of cells. Change in the charges of surfaces might play a key role in the binding ability of cells. As mentioned above, APTMS-treated substrates have positively charged surfaces because of protonation of amine groups. The silanol groups on the surface of bare glass coverslip are deprotonated under the condition of cell culture. As a result, the surface is negatively charged. Cells cultured on the silica beads are attached weakly on the substrate, and the migration is much

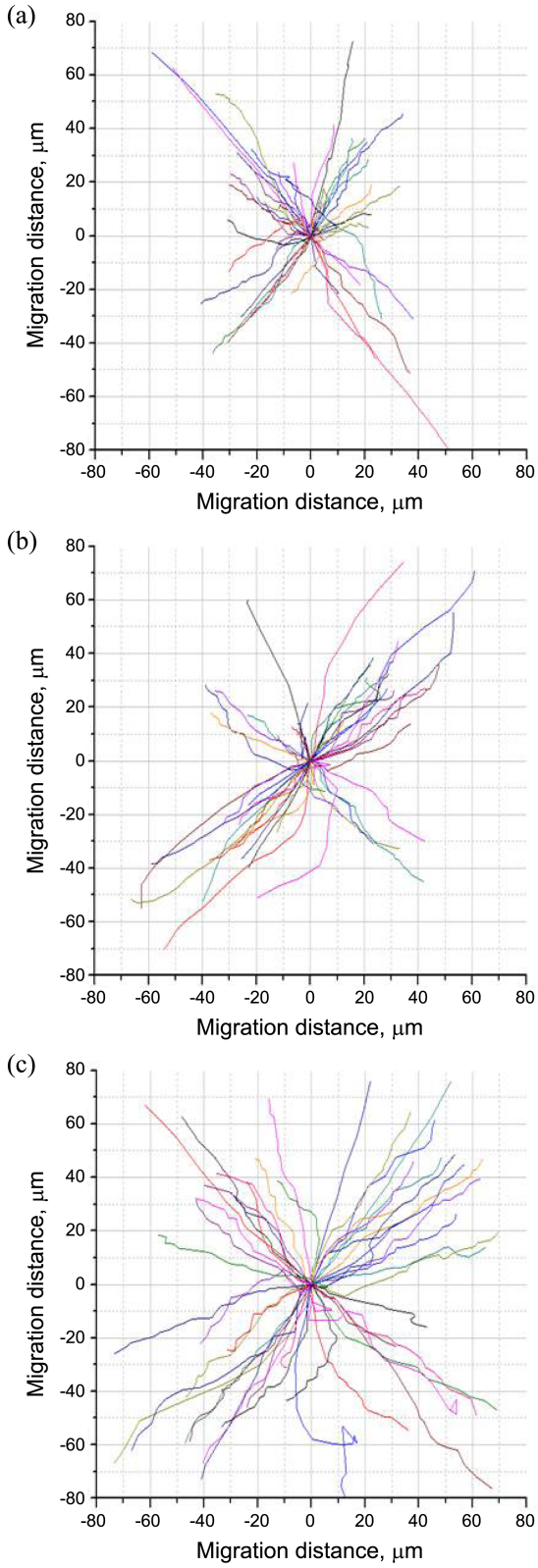

Figure 4. Superimposed migration tracks of 50 randomly selected cells cultured on three different surfaces, (a) bare glass coverslip, (b) APTMS-treated coverslip, and (c) silica beads-treated coverslip. The cells with a density of 1×10^5 cells/mL were loaded on the substrates placed in the 6-well plate, and cultured on the motorized stage of an inverted microscope. The cell migration was monitored by capture of time-lapse images of cells for 1 h with an interval of 1 min.

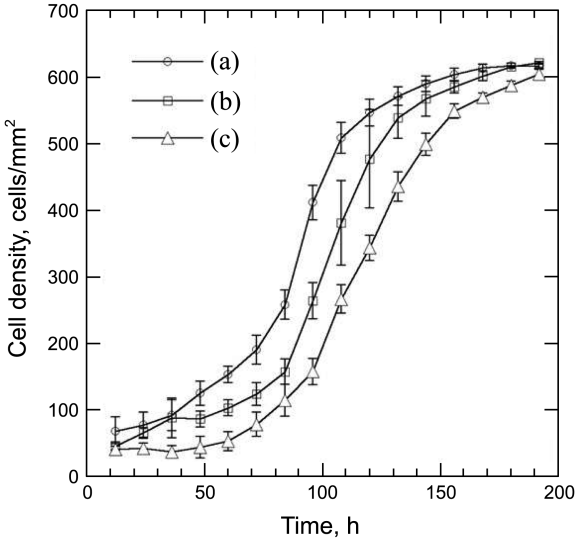

Figure 5. Cell growth curves of BALB/3T3 fibroblast cells on three different surfaces for 192 h, (a) bare glass coverslip, (b) APTMS-treated coverslip, and (c) silica beads-treated coverslip. The cells with a density of 1×10^2 cells/mm^2 were loaded on the substrates placed in the 6-well plate, and cultured in the humidified incubator. Images were collected at a regular interval of 12 h, and the numbers of cells were counted by image analyses software.

faster than on bare glass. Because the close-packed silica beads array gave embossed surfaces, the contact area between cells and surface is lower than those of other smooth substrates. The binding ability of cells on the substrates is the main reason for the difference in the cell migration.

Adhesion and Proliferation of Balb/3T3 Fibroblast Cells on the Substrates. Adhesion and proliferation of cells on the substrates were analyzed with the live cell imaging system using Image-pro software. Cells were loaded on the substrates with the same initial cell densities (~100 cells/mm^2) and ten experiments were carried out for each condition for a quantitative analysis with reproducibility. Cells were attached, spread, and proliferated on the substrates. Culture media were not replaced during the experiments. The growth curves were plotted and the proliferation rates were measured for the substrates as shown in Figure 5.

The growth curves are typical S-shaped ones. The growth rates of cells on the substrates were affected by topology and charge of the surfaces. The growth rates of cells on the silica beads were somewhat lower than those of the control glass coverslip or APTMS-treated substrate, because cells were weakly attached on the substrate. The times to reach the 50% confluence were 84 h on the bare glass, 96 h on the APTMS treated glass, and 108 h on the silica beads. In the case of the silica bead surface, the surface is neither smooth nor flat. The cells attached only on the ridge region of close-packed silica beads with spacing of 550 nm and they did not attached to the groove regions. The binding of cells on the surface was very weak compared to the smooth bare glass and APTMS coated surface. The cytoskeleton controls the mechanotransduction which influences the vital functions of

cells like growth, proliferation, migration, and gene expression. Mechanotransduction responds to the conformational change in the cytoskeleton and passes chemical and mechanical signals to the nucleus about the extracellular environment.[32,33] Attachment of cells to the substrates or other cells has long been implicated in cell cycle regulation. During cell division, the cells undergo extensive cell shape changes to detach from and reattach to the substrate. Changes in gross morphology and contact guidance over microstructured surfaces may result in cell cycle arrest or may slow down the cell cycle.[34] It could be speculated that microstructure reduced adhesion, and it impacts on integrin-related signaling through the reduction of sites for adhesion and cytoskeletal anchorage. This further reduced tension applied to the cell from a well-organized extracellular matrix *via* the cytoskeleton to the nucleus, effectively shutting the cells down to transcription, leading to a reduced growth rate.

Cytoskeletal Depolymerization and Nuclear Condensation. To determine the effects of topology and surface charge of substrate on cytoskeleton organization and nuclear structure of the cell, F-actin (actin filaments) and DNA of the nucleus were stained simultaneously after culture. Fluorescent microscopic images of immunocytochemical stained cytoskeleton and nucleus of cells cultured on three different surfaces are shown in Figure 6. In control, the actin filaments were well organized in thickened longitudinal bundles forming stress fibers in control cells (Figure 6(a)). In addition, examination of DAPI staining revealed morphological changes in the nuclei of cells cultured on the silica beads as compared to controls. Most stained nuclei in controls were healthy and morphologically oval-shaped with diffuse chromatin distribution (Figure 6(a)). Cells cultured on the APTMS coated substrate (Figure 6(b)) show slight changes in their actin filaments, or nuclei as compared to the control cells. Actin filaments became fragmented, thinner, and disorganized in cells. Nuclei were slightly shrunken and irregularly shaped. The functional groups of substrate can be charged differently; the silanol groups are negatively chargeable and the amine groups are positively chargeable. Slight changes in the cytoskeleton organization and nuclear structure of the cell are probably due to the alteration of surface charge. However, in the case of cells cultured on the silica beads array, actin filaments were thinner, disorganized, and fragmented, and formed knots at regular intervals in the treated cells (Figure 6(c)). In addition, nuclei of cells cultured on the silica beads were irregularly shaped, highly shrunken, and exhibited chromatin condensation as a characteristic feature of unhappy nuclei (Figure 6(c)). Arrows indicate significant differences in their organization when compared to respective controls. As the weak binding of cells on the substrates induced the retardation of actin formation, the cytoskeleton disorganization and nuclear condensation occurred.

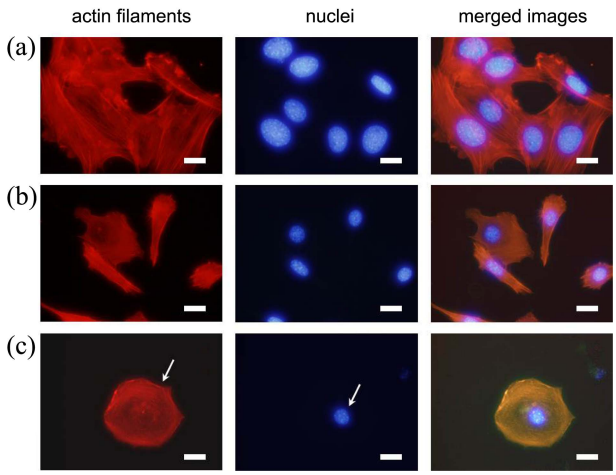

Figure 6. Fluorescent microscopic images of immunocytochemical stained cytoskeleton and nucleus of cells cultured on three different surfaces for 24 h. (a) bare glass coverslip, (b) APTMS-treated coverslip, and (c) silica beads-treated coverslip. Cells were cultured for 24 h on the substrates and stained for F-actin (actin filaments) and nuclei. Arrows indicate significant differences in their organization when compared to respective controls. Data shown are representative of three independent experiments. Scale bars: 10 μm.

Conclusion

APTMS treated silica beads synthesized using the modified Stöber method were immobilized on the TESPSA treated glass coverslip, and a close-packed silica beads surface was obtained. Cells were cultured on the bare glass, APTMS treated coverslip, and APTMS treated silica beads. Because the close-packed silica beads array gave embossed surfaces, the contact area between cells and surface is lower than those of other smooth substrates. Cells cultured on the silica beads showed faster migration and slower proliferation than those on other smooth substrates. The binding ability of cells on the substrates is the main reason for the difference in the cell migration and proliferation. Furthermore, the nuclei of the cells cultured on the silica beads were irregularly shaped, highly shrunken and exhibited chromatin condensation. The cytoskeleton disorganization and nuclear condensation, which were probably induced by the weak binding of cells on the embossed surfaces were observed. The results described here are very important in the understanding of the interaction between implanted materials and biosystems.

Acknowledgments. This research was supported by the Basic Science Research Program (2013R1A1A2010198) and Priority Research Centers Program (2012-0006682) through the National Research Foundation of Korea (NRF) funded by the Ministry of Education.

References

1. Ratner, B. D.; Bryant, S. J. *Annu. Rev. Biomed. Eng.* **2004**, *6*, 41.
2. Chen, C. S.; Mrksich, M.; Huang, S.; Whitesides, G. M.; Ingber, D. E. *Science* **1997**, *276*, 1425.
3. Curtis, A.; Wilkinson, C. *Biomaterials* **1997**, *18*, 1573.
4. Chen, W.; Villa-Diaz, L. G.; Sun, Y.; Weng, S.; Kim, J. K.; Lam, R. H. W.; Han, L.; Fan, R.; Krebsbach, P. H.; Fu, J. *ACS Nano* **2012**, *6*, 4094.
5. Taborelli, M.; Jobin, M.; François, P.; Vaudaux, P.; Tonetti, M.;

Szmukler-Moncler, S.; Simpson, J. P.; Descouts, P. *Clin. Oral Impl. Res.* **1997**, *8*, 208.
6. Ehrenfest, D. M. D.; Coelho, P. G.; Kang, B.-S.; Sul, Y.-T.; Albrektsson, T. *Trends Biotechnol.* **2010**, *28*, 198.
7. Wennerberg, A.; Albrektsson, T.; Johansson, C.; Andersson, B. *Biomaterials* **1996**, *17*, 15.
8. Lehnert, D.; Wehrle-Haller, B.; David, C.; Weiland, U.; Ballestrem, C.; Imhof, B. A.; Bastmeyer, M. *J. Cell Sci.* **2004**, *117*, 41.
9. Xia, Y.; Whitesides, G. M. *Annu. Rev. Mater. Sci.* **1998**, *28*, 153.
10. Lamers, E.; te Riet, J.; Domanski, M.; Luttge, R.; Figdor, C. G.; Gardeniers, J. G. E.; Walboomers, X. F.; Jansen, J. A. *Eur. Cell. Mater.* **2012**, *23*, 182.
11. Lord, M. S.; Foss, M.; Besenbacher, F. *Nano Today* **2010**, *5*, 66.
12. Tan, J. L.; Tien, J.; Pirone, D. M.; Gray, D. S.; Bhadriraju, K.; Chen, C. S. *Proc. Natl. Acad. Sci. USA* **2003**, *100*, 1484.
13. Bettinger, C. J.; Langer, R.; Borenstein, J. T. *Angew. Chem. Int. Ed. Engl.* **2009**, *48*, 5406.
14. Hickman, G. J.; Rai, A.; Boocock, D. J.; Rees, R. C.; Perry, C. C. *J. Mater. Chem.* **2012**, *22*, 12141.
15. Barandeh, F.; Nguyen, P.-L.; Kumar, R.; Iacobucci, G. J.; Kuznicki, M. L.; Kosterman, A.; Bergey, E. J.; Prasad, P. N.; Gunawardena, S. *PLoS ONE* **2012**, *7*, e29424.
16. Rampazzo, E.; Brasola, E.; Marcuz, S.; Mancin, F.; Tecilla, P.; Tonellato, U. *J. Mater. Chem.* **2005**, *15*, 2687.
17. Cousins, B. G.; Doherty, P. J.; Williams, R. L.; Fink, J.; Garvey, M. J. *J. Mater. Sci.: Mater. Med.* **2004**, *15*, 355.
18. Lamers, E.; van Horssen, R.; te Riet, J.; van Delft, F. C. M. J. M.; Luttge, R.; Walboomers, X. F.; Jansen, J. A. *Eur. Cell. Mater.* **2010**, *20*, 329.
19. Lipski, A. M.; Pino, C. J.; Haselton, F. R.; Chen, I.-W.; Shastri, V. P. *Biomaterials* **2008**, *29*, 3836.
20. Lipski, A. M.; Jaquiery, C.; Choi, H.; Eberli, D.; Stevens, M.; Martin, I.; Chen, I.-W.; Shastri, V. P. *Adv. Mater.* **2007**, *19*, 553.
21. Stöber, W.; Fink, A.; Bohn, E. *J. Colloid Interf. Sci.* **1968**, *26*, 62.
22. Zhang, H.; Wu, J.; Zhou, L.; Zhang, D.; Qi, L. *Langmuir* **2007**, *23*, 1107.
23. Chen, S.-L.; Yuan, G.; Hu, C.-T. *Powder Technol.* **2011**, *207*, 232.
24. Jung, H.-S.; Moon, D.-S.; Lee, J.-K. *J. Nanomater.* **2012**, 593471.
25. Rahman, I. A.; Padavettan, V. *J. Nanomater.* **2012**, 132424.
26. Barabanova, A. I.; Pryakhina, T. A.; Afanas'ev, E. S.; Zavin, B. G.; Vygodskii, Ya. S.; Askadskii, A. A.; Philippova, O. E.; Khokhlov, A. R. *Appl. Surf. Sci.* **2012**, *258*, 3168.
27. Taira, S.; Kaneko, D.; Onuma, K.; Miyazato, A.; Hiroki, T.; Kawamura-Konishi, Y.; Ichiyanagi, Y. *Int. J. Inorg. Chem.* **2012**, 439751.
28. Karunakaran, R. G.; Lu, C.-H.; Zhang, Z.; Yang, S. *Langmuir* **2011**, *27*, 4594.
29. Rhee, S. W.; Taylor, A. M.; Tu, C. H.; Cribbs, D. H.; Cotman, C. W.; Jeon, N. L. *Lab Chip* **2005**, *5*, 102.
30. Webb, K.; Hlady, V.; Tresco, P. A. *J. Biomed. Mater. Res.* **1998**, *41*, 422.
31. Manifar, T.; Rezaee, A.; Sheikhzadeh, M.; Mittler, S. *Appl. Surf. Sci.* **2008**, *254*, 4611.
32. Dalby, M. J. *Int. J. Nanomedicine* **2007**, *2*, 373.
33. Dalby, M. J. *Med. Eng. Phys.* **2005**, *27*, 730.
34. Lee, K.; Song, K. *Cell Cycle* **2007**, *6*, 1487.